



**HAL**  
open science

# Synthesis and Self-Assembly of Hydroxypropyl Methyl Cellulose-block-Poly( $\epsilon$ -caprolactone) Copolymers as Nanocarriers of Lipophilic Drugs

Aijing Lu, Eddy Petit, Yuandou Wang, Feng Su, Suming Li

► **To cite this version:**

Aijing Lu, Eddy Petit, Yuandou Wang, Feng Su, Suming Li. Synthesis and Self-Assembly of Hydroxypropyl Methyl Cellulose-block-Poly( $\epsilon$ -caprolactone) Copolymers as Nanocarriers of Lipophilic Drugs. ACS Applied Nano Materials, 2020, 3 (5), pp.4367-4375. 10.1021/acsanm.0c00498 . hal-02946336

**HAL Id: hal-02946336**

**<https://hal.science/hal-02946336>**

Submitted on 25 May 2023

**HAL** is a multi-disciplinary open access archive for the deposit and dissemination of scientific research documents, whether they are published or not. The documents may come from teaching and research institutions in France or abroad, or from public or private research centers.

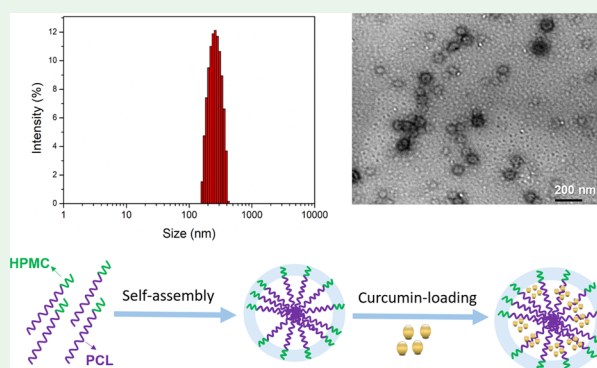
L'archive ouverte pluridisciplinaire **HAL**, est destinée au dépôt et à la diffusion de documents scientifiques de niveau recherche, publiés ou non, émanant des établissements d'enseignement et de recherche français ou étrangers, des laboratoires publics ou privés.

# Synthesis and Self-Assembly of Hydroxypropyl Methyl Cellulose-*block*-Poly( $\epsilon$ -caprolactone) Copolymers as Nanocarriers of Lipophilic Drugs

Aijing Lu, Eddy Petit, Yuandou Wang, Feng Su, and Suming Li\*

**ABSTRACT:** A series of amphiphilic diblock copolymers with different hydrophilic and hydrophobic block lengths were synthesized by reductive amination of hydroxypropyl methyl cellulose (HPMC) and end-functionalized poly( $\epsilon$ -caprolactone) (PCL). NH<sub>2</sub>-PCL was synthesized by ring-opening polymerization of  $\epsilon$ -caprolactone using 3-(Boc-amino)-1-propanol as the initiator, followed by removal of the Boc group with trifluoroacetic acid treatment. Proton NMR, DOSY-NMR, Fourier transform infrared, and the Kaiser test confirmed the successful synthesis of HPMC–PCL diblock copolymers. The copolymers were able to self-assemble by dissolution in water, yielding spherical nanoscale micelles of *ca.* 200 nm, as revealed by transmission electron microscopy and dynamic light scattering. The micelle size was mainly dependent on the hydrophilic HPMC block length. The longer the HPMC block, the larger the micelle size. The critical micelle concentration determined by fluorescence spectroscopy decreased with the increasing hydrophobic PCL block length. Curcumin was loaded in copolymer micelles as a lipophilic antitumor drug. Higher drug loading was obtained for copolymers with longer PCL blocks. The *in vitro* drug release profile consisted two phases with an initial burst and a subsequent slower release. Faster drug release is observed for copolymers with a shorter PCL block length and lower drug loading. HPMC–PCL copolymer micelles exhibited outstanding cytocompatibility, as evidenced by the MTT test using L929 cells. Therefore, it is concluded that biodegradable and biocompatible HPMC–PCL block copolymers present great potential as nanocarriers of lipophilic antitumor drugs.

**KEYWORDS:** hydroxypropyl methyl cellulose, poly( $\epsilon$ -caprolactone), block copolymer, reductive amination, micelle, self-assembly, drug release



## 1. INTRODUCTION

In the past decades, polymeric nanomicelles have attracted increasing attention as drug delivery systems because of their unique advantages including enhanced drug solubility, prolonged blood circulation, passive targeting to tumor tissue by enhanced permeability and retention effect, decreased adverse effects, and improved drug bioavailability.<sup>1</sup> Micelles are generally prepared from amphiphilic block copolymers via various self-assembly approaches. The hydrophobic component aggregates into the core which is capable of encapsulating lipophilic drugs, whereas the hydrophilic component forms the shell to stabilize the micelle structure in an aqueous medium. Generally, amphiphilic copolymers used in drug delivery should be biocompatible, bioresorbable, and nontoxic as they should be metabolized in or excreted from the human body without causing adverse reactions.

Poly( $\epsilon$ -caprolactone) (PCL) is an FDA-approved biocompatible and biodegradable polyester which has been extensively studied as drug carriers, medical implants, and tissue engineering scaffolds.<sup>2</sup> In drug delivery, many PCL-based

formulations have been investigated, including nanoparticles, nanofibers, hydrogels or nanogels, polymersomes, micelles, polyplexes, and drug-conjugates.<sup>3</sup> In fact, PCL can be used as a degradable and hydrophobic block to combine with various hydrophilic polymers, including both natural biopolymers such as starch,<sup>4</sup> and chitosan,<sup>5,6</sup> and synthetic polymers such as poly(ethylene glycol) (PEG),<sup>3</sup> polyurethane (PU),<sup>7</sup> and so forth. Importantly, PCL is compatible with a wide range of drugs.<sup>8,9</sup> It has been reported that PCL-based micelles can encapsulate doxorubicin,<sup>10,11</sup> 5-fluoro uracil,<sup>12</sup> curcumin,<sup>6</sup> paclitaxel,<sup>13</sup> nimodipine,<sup>14</sup> sorafenib,<sup>15</sup> and so forth. Among them, curcumin has received much attention in the past

decades because it is a naturally occurring polyphenol with outstanding biological activities, including anticancer, anti-inflammatory, antibiotic, antioxidant, and antiviral activities.<sup>16,17</sup>

As a hydrophilic polymer, polysaccharides including cellulose, chitosan, alginate, dextran, cyclodextrin, and so forth have attracted widespread interest because of their biocompatibility, biodegradability, nontoxicity, and the presence of numerous hydroxyl groups allowing chemical modification.<sup>18</sup> Cellulose is the most abundant polysaccharide which is a linear  $\beta$ -1,4-glucan with an acetal linkage between C1 and C4 carbon atoms.<sup>19</sup> Cellulose is insoluble in water and in common organic solvents, but it can be dissolved in *N*-methylmorpholine *N*-oxide, ionic liquids, or in water at extreme pHs. The poor solubility of cellulose is referred to strong intrachain and interchain hydrogen bonding. The intrachain hydrogen bonding is dominated by the strong O3–H...O5 bond which is responsible for the high axial chain stiffness, whereas the interchain hydrogen bonding ensures the cohesion between cellulose chains.<sup>20</sup> This poor solubility greatly restrains the potential applications of cellulose for the synthesis of amphiphilic copolymers. Chemical modification of cellulose is performed by substitution of hydroxyl groups with alkyl or hydroxyalkyl ones so as to reduce the hydrogen bonding and thus to improve the solubility. A number of water soluble derivatives of cellulose are commercially available, including hydroxyethyl cellulose, carboxymethyl cellulose, ethyl cellulose, hydroxypropyl cellulose, and hydroxypropyl methyl cellulose (HPMC).<sup>21</sup>

As a biobased polymer, HPMC has been widely used in pharmaceutical and food preparations such as viscolizing or thickening agent, coating polymer, bioadhesive, capsule shell, excipient, and eyedrops. It is one of the most important hydrophilic biopolymers used in oral drug delivery because of its high swellability.<sup>22</sup> Controlled radical polymerization based on hydroxyl groups has been used to synthesize graft copolymers. Bordallo *et al.* synthesized a series of oxidized carboxymethyl cellulose-graft-poly(ethylene glycol)-dodecylamine (OCMC-*g*-PEG-DDA) with different contents of DDA.<sup>23</sup> The copolymers are able to form micelles with narrow size distribution. Wang *et al.* synthesized ethyl cellulose-graft-poly(2-(diethylamino) ethyl methacrylate) (EC-*g*-PDEAE-MA).<sup>24</sup> pH-responsive micelles are obtained from the copolymers which can efficiently encapsulate rifampicin. Das and Pal evaluated hydroxypropyl methyl cellulose-graft-polyacrylamide (HPMC-*g*-PAM) as a potential carrier of 5-amino salicylic acid.<sup>25</sup> However, grafting polymerization is poorly controllable because of the large number of hydroxyl groups on the polymer backbone. In contrast, water soluble cellulose derivatives can be used as a hydrophilic component for the preparation of amphiphilic block copolymers because the reducing end (hemiacetal group) of cellulose is easily converted to an aldehyde group. Reductive amination between aldehyde and amino groups is a well-established reaction but is rarely used to synthesize cellulose-based block copolymers because of the lack of common solvent for the two blocks, side reactions induced by lateral hydroxyl groups, and limited availability of the hemiacetal group at the chain end.

In our previous work, linear HPMC–polylactide (HPMC–PLA) and Y-type (HPMC)<sub>2</sub>–PLA block copolymers were synthesized for the first time by combination of ring-opening polymerization (ROP), amination reduction and UV initiated thiol-ene or thiol-yne click reaction.<sup>26,27</sup> More recently,

reductive amination was used to synthesize HPMC–PLA diblock copolymers and HPMC–JEFFAMINE diblock, triblock, and three-armed copolymers.<sup>28,29</sup> These various amphiphilic and thermo-responsive copolymers are able to aggregate in micelles by self-assembly in an aqueous medium and serve as nanocarriers of lipophilic drugs. In this work, amino-terminated PCL (NH<sub>2</sub>-PCL) was prepared by ROP of  $\epsilon$ -caprolactone using *tert*-butyl-*N*-(3-hydroxypropyl) carbamate as initiator, followed by removal of the *N*-*tert*-butoxycarbonyl (Boc) group. HPMC–PCL block copolymers with different PCL and HPMC block lengths were then synthesized by reductive amination between the amine of NH<sub>2</sub>-PCL and the hemiacetal end of HPMC. The self-assembly, drug loading and drug release behaviors, and the biocompatibility of HPMC–PCL copolymers were investigated to evaluate their potential as nanocarriers of lipophilic drugs in cancer therapy.

## 2. EXPERIMENTAL SECTION

**2.1. Materials.**  $\epsilon$ -Caprolactone was purchased from Aldrich and purified by distillation under reduced pressure. HPMC was provided by Dow Colorcon Limited France, and HPMC oligomers with  $M_w$  of 7000 and 18,000 Da were prepared by enzymatic degradation, as reported in our previous work.<sup>26,27</sup> *tert*-Butyl-*N*-(3-hydroxypropyl) carbamate (3-(Boc-amino)-1-propanol), sodium triacetoxyborohydride (NaBH(OAc)<sub>3</sub>), tin(II) 2-ethylhexanoate (Sn(Oct)<sub>2</sub>), anhydrous dimethyl sulfoxide (DMSO), and curcumin were purchased from Sigma-Aldrich and used without further purification. Trifluoroacetic acid (TFA) was purchased from Merck KGaA. Dichloromethane was purchased from Sigma-Aldrich, dried by anhydrous calcium chloride (CaCl<sub>2</sub>), and distilled before use.

**2.2. Synthesis of End-Functionalized PCL.** End-functionalized PCL was prepared by ROP of  $\epsilon$ -caprolactone in the presence of 3-(Boc-amino)-1-propanol as initiator and Sn(Oct)<sub>2</sub> as catalyst, followed by treatment with TFA to remove the Boc group.<sup>30,31</sup> Typically, 0.35 g of 3-(Boc-amino)-1-propanol (2 mmol), 4.56 g of  $\epsilon$ -caprolactone (40 mmol), and 0.0932 g of Sn(Oct)<sub>2</sub> (2.3 mmol) were added into a dried Schlenk flask. Three freeze–pump–thaw cycles were required to degas the mixture, and the reaction proceeded at 120 °C for 24 h. Boc-NH-PCL was then obtained as a white powder using the dissolution/precipitation method. Subsequently, the Boc group of Boc-NH-PCL was removed with TFA treatment using the previously reported method.<sup>29</sup>

**2.3. Synthesis of HPMC–PCL Block Copolymers.** Reductive amination was performed to synthesize HPMC–PCL block copolymers.<sup>32,33</sup> Briefly, 0.16 g of NH<sub>2</sub>-PCL (0.154 mmol), 1.0 g of HPMC (0.14 mmol) with  $M_w$  of 7000, and 0.042 g of NaBH(OAc)<sub>3</sub> (0.2 mmol) were added in 20 mL of anhydrous DMSO under stirring. After complete dissolution, the reaction proceeded 72 h at 35 °C under a nitrogen atmosphere. The final product was obtained by 72 h dialysis in deionized water, followed by 48 h freeze-drying.

**2.4. Characterization.** <sup>1</sup>H NMR was performed on a 300 MHz Bruker spectrometer (AVANCE300), and diffusion ordered spectroscopy (DOSY) NMR was performed on a 400 MHz Bruker AVANCE spectrometer (AQS400) equipped with a Bruker multinuclear z-gradient inverse probe head. CDCl<sub>3</sub>, DMSO-*d*<sub>6</sub> and D<sub>2</sub>O were used as solvent. <sup>1</sup>H NMR spectra were processed by using MestReNova software, and DOSY NMR spectra were processed by using Bruker Topspin and Dosy Toolbox software.

The Kaiser test was performed using Kaiser test kit from Sigma-Aldrich containing KCN in H<sub>2</sub>O/pyridine (Reagent A), 6% ninhydrin in ethanol (Reagent B), and 80% phenol in ethanol (Reagent C). A small amount of polymer was added into a test tube, followed by successive addition of two or three drops of Reagent A, B, and C. Then, the tube was heated at 110 °C for 5 min. The solution color was finally compared to that of the control without addition of the polymer. The tests were performed in triplicate.

Gel permeation chromatography (GPC) was performed on a Viscotek TDA 305 multidetector GPC/SEC system using THF as the mobile phase and polystyrene standards (Polysciences, Warrington, PA) for calibration. Polymer solutions at 10 g/L were filtered through a 0.22  $\mu\text{m}$  Millipore filter before injection.

Fourier transform infrared (FT-IR) was performed on a Nicolet NEXUS spectrometer with attenuated total reflection accessory. Spectra were recorded in the range from 650 to 4000  $\text{cm}^{-1}$  with a resolution at 4  $\text{cm}^{-1}$ . Thirty two scans were performed for each analysis.

Dynamic light scattering (DLS) was carried out on Anton Parr Litesizer 500 at 25  $^{\circ}\text{C}$ . Micelle solutions were prepared at a concentration of 1.0  $\text{mg mL}^{-1}$  and filtered through a 0.45  $\mu\text{m}$  cellulose acetate (CA) filter. All measurements were performed at a scattering angle of 90 $^{\circ}$ .

The critical micelle concentration (CMC) of copolymers was determined by fluorescence spectroscopy using pyrene as probe. An aqueous pyrene solution ( $6 \times 10^{-7}$  g/L) was used to prepare copolymer solutions at concentrations ranging from  $1.0 \times 10^{-4}$  to 2.0 mg/mL. The excitation spectra of the pyrene solutions were registered in the 300–360 nm range at an excitation wavenumber of 395 nm.

Transmission electron microscopy (TEM) was carried out on JEOL 1400 plus instrument at an accelerating voltage of 120 kV. Samples at 1.0  $\text{mg mL}^{-1}$  were dropped on a carbon-coated copper grid and stained by exposure to ruthenium oxide vapor for 7 min. Ruthenium(VIII) oxide solution was prepared as follows: sodium periodate (2.0 g) was added in water (50 g), and then, ruthenium(IV) oxide (0.30 g) was added in the solution under stirring at room temperature, yielding a yellow solution of ruthenium(VIII) oxide.<sup>34,35</sup>

**2.5. In Vitro Drug Release.** Drug-loaded micelles were prepared using a previously reported method.<sup>29</sup> Blank micelles were first prepared by dissolution of 20 mg of copolymer in 20 mL of distilled water. Curcumin (2 mg) was dissolved in 400  $\mu\text{L}$  of ethanol, and the solution was then dropped into the micelle solution under vigorous stirring. The solvent was evaporated overnight, yielding a drug-loaded micelle solution. The solution was filtered through 0.8  $\mu\text{m}$  CA filter to eliminate unloaded drug, lyophilized, and stored at 4  $^{\circ}\text{C}$  before analysis.

*In vitro* drug release was realized by using Float-A-Lyzer G2 dialysis devices with MWCO of 3 500 Da, as previously reported.<sup>29</sup> Briefly, 1 mL of drug-loaded micelle solution at 2.0 mg/mL was added in a dialysis device which was placed in a tube containing 40 mL of phosphate buffered saline (PBS). The release medium was regularly renewed to ensure sink conditions. Drug release was performed in a water bath at 37  $^{\circ}\text{C}$  under constant shaking. An aliquot of 25  $\mu\text{L}$  solution was collected from the dialysis device at each data point, and the same volume of fresh PBS was added.

HPLC–MS was used to determine the concentration of curcumin in solution, using a 50/50 v/v mixture of acetonitrile and pH 7.4 PBS as the mobile phase. Drug loading content (DLC) and drug loading efficiency (DLE) were determined from the following equations<sup>36</sup>

$$\text{DLC} = \frac{\text{weight of loaded drug}}{\text{weight of polymeric micelles}} \times 100\% \quad (1)$$

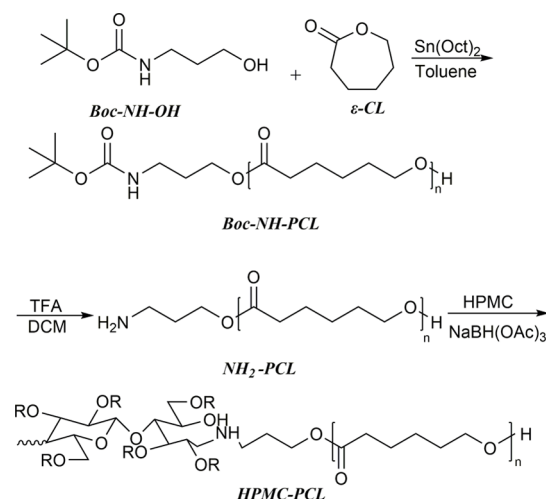
$$\text{DLE} = \frac{\text{weight of loaded drug}}{\text{theoretical drug loading}} \times 100\% \quad (2)$$

**2.6. MTT Assay.** MTT assay was performed to evaluate the biocompatibility of HPMC–PCL micelles on L-929 cells, as previously reported.<sup>29</sup>

### 3. RESULTS AND DISCUSSION

**3.1. Synthesis and Characterization of Amphiphilic Copolymers.** Amphiphilic HPMC–PCL block copolymers were synthesized in three steps, as shown in Scheme 1. Boc-NH<sub>2</sub>-PCL was first synthesized by ROP of  $\epsilon$ -caprolactone initiated by 3-(Boc-amino)-1-propanol which has a protected

#### Scheme 1. Synthesis of HPMC–PCL Block Copolymers via Reductive Amination



amine group and a hydroxyl endgroup. The Boc group was then removed with TFA treatment to obtain end functionalized PCL. HPMC–PCL block copolymers were finally obtained via reductive amination between the hemiacetal endgroup of HPMC and the amine group of PCL in the presence of  $\text{NaBH}(\text{OAc})_3$  as the reducing agent.<sup>37</sup>

The synthesis of amino terminated NH<sub>2</sub>-PCL was based on the method reported in literature.<sup>38,39</sup> Boc-NH-PCL was first synthesized by ROP of  $\epsilon$ -caprolactone with predetermined monomer/initiator (M/I) molar ratios of 10, 20, or 30. The obtained polymers were characterized by FT-IR, GPC, and quantitative <sup>1</sup>H NMR. As shown in Figure 1A, the signals at

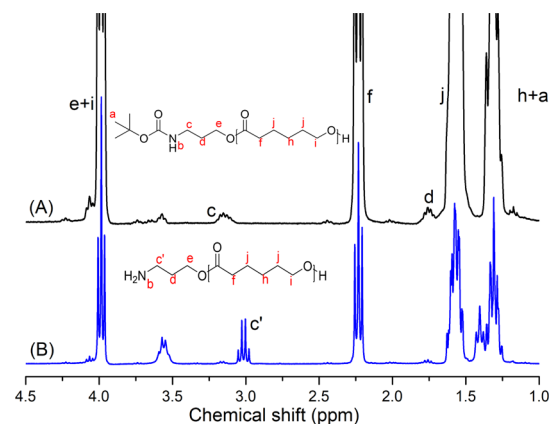


**Figure 1.** <sup>1</sup>H NMR spectra of Boc-NH-PCL<sub>10</sub> (A) and NH<sub>2</sub>-PCL<sub>10</sub> (B) in CDCl<sub>3</sub>.

1.42 (a), 4.18 (e), 1.84 (d), and 3.20 (c) ppm belong to the methyl and the methylene protons of the terminal Boc group, respectively, and the signals at 1.30 (h), 1.62 (j), 2.75 (f), and 4.0 (i) ppm are assigned to the methylene protons of the PCL backbone. The degree of polymerization (DP) of PCL was estimated from the integration ratio of signals f to c. The obtained DP<sub>PCL</sub> is 10.8, 22.4, and 30.5, which is rather close to the monomer/initiator ratio. The number average molar mass ( $M_{n,NMR}$ ) was calculated from the DP values. It varied from 1320 to 3600, as shown in Table S1.

**Table 1. Self-Assembly and Drug Loading Properties of HPMC–PCL Block Copolymers**

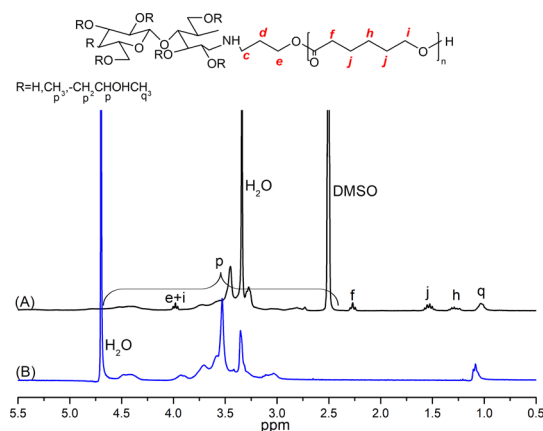
sample	size (nm)	PDI	ZETA (mV)	CMC (mg/mL)	DLC (%)	DLE (%)
HPMC7K-PCL <sub>10</sub>	179.0 ± 2.1	0.16	-4.5 ± 0.3	0.012	4.3	41.5
HPMC7K-PCL <sub>20</sub>	182.8 ± 1.2	0.17	-2.3 ± 0.4	0.0058	5.1	48.2
HPMC7K-PCL <sub>30</sub>	195.9 ± 2.5	0.12	-6.7 ± 0.2	0.0009	8.2	75.8
HPMC18K-PCL <sub>10</sub>	205.1 ± 3.4	0.19	-6.8 ± 0.2	0.009	3.8	36.4
HPMC18K-PCL <sub>20</sub>	216.9 ± 1.3	0.16	-8.9 ± 0.4	0.005	4.4	41.7
HPMC18K-PCL <sub>30</sub>	222.0 ± 3.0	0.11	-5.4 ± 0.2	0.003	7.2	67.0

The molar mass and dispersity ( $\mathcal{D} = M_w/M_n$ ) of polymers were determined by GPC, as shown in Figure S1A. A symmetric molar mass distribution is observed. The  $M_{n, \text{GPC}}$  increases from 3180 to 5140 with the increase of  $DP_{\text{PCL}}$  from 10 to 30, whereas the dispersity ranges from 1.29 to 1.41 (Table S1). The  $M_{n, \text{GPC}}$  values are larger than those from NMR. The difference can be assigned to the fact that  $M_{n, \text{GPC}}$  is obtained from the hydrodynamic volume of polymer chains in solution compared to that of polystyrene standards, in contrast to  $M_{n, \text{NMR}}$  values which are calculated from the integrations of NMR signals.

$\text{NH}_2$ -PCL was obtained by treating Boc-NH-PCL with TFA to remove the Boc group. As shown in Figure S1, Boc-NH-PCL<sub>30</sub> and  $\text{NH}_2$ -PCL<sub>30</sub> present almost the same elution time. In other words, deprotection by TFA treatment did not cleave PCL chains.  $^1\text{H}$  NMR was performed to evidence the effective removal of the Boc group (Figure 1B). The methyl peak (a) of Boc at 1.42 ppm is not detected on the spectrum of  $\text{NH}_2$ -PCL<sub>10</sub>. Meanwhile, the methylene peak (c) shifts from 3.2 ppm for Boc-NH-PCL<sub>10</sub> to 3.0 ppm for  $\text{NH}_2$ -PCL<sub>10</sub> (c'), in agreement with the conversion of the adjacent acylamino group to the amine group. The intensity ratio between signals c and f remains constant, thus confirming the absence of PCL chain degradation during deprotection.

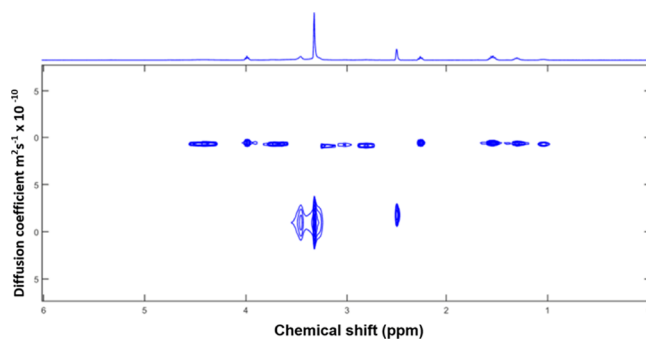
The Kaiser test is commonly utilized to evidence the presence of primary amines. The main effective constituent of the Kit, ninhydrin, reacts with amine groups to produce an intense blue color. As shown in Figure S1B, Boc-NH-PCL presents almost the same color as the control, while  $\text{NH}_2$ -PCL solution is dark blue. This finding demonstrates the presence of primary amino groups in  $\text{NH}_2$ -PCL but not in Boc-NH-PCL.

Finally, amphiphilic HPMC–PCL block copolymers were synthesized by reductive amination of  $\text{NH}_2$ -PCL and HPMC in the presence of a reducing agent,  $\text{NaBH}(\text{OAc})_3$ . Six HPMC–PCL copolymers were obtained in this work, namely, HPMC7K-PCL<sub>10</sub>, HPMC7K-PCL<sub>20</sub>, HPMC7K-PCL<sub>30</sub>, HPMC18K-PCL<sub>10</sub>, HPMC18K-PCL<sub>20</sub>, and HPMC18K-PCL<sub>30</sub> (Table 1). As shown in Figure 2A, the  $^1\text{H}$  NMR spectrum of HPMC7K-PCL<sub>10</sub> in  $\text{DMSO}-d_6$  presents a signal at 1.05 ppm (q) assigned to methyl protons of the hydroxypropyl substitution group, signals between 2.75 and 4.75 ppm (p) corresponding to the methylene and methine protons of the substitution group, methyl protons adjacent to the oxygen moieties of ether linkage, and the protons of glucose units of HPMC. The signals at 1.30 (h), 1.62 (j), 2.75 (f), and 4.0 (i) ppm belong to the methylene protons of PCL blocks. The Kaiser test also corroborates with the effective reductive amination (Figure S1B). In fact, HPMC–PCL almost shows the same color as the control, indicating the absence of primary amines. In other words, all the terminal amino groups of  $\text{NH}_2$ -PCL<sub>30</sub> have reacted with aldehyde groups of HPMC.

**Figure 2.**  $^1\text{H}$  NMR spectra of HPMC7K-PCL<sub>10</sub> in  $\text{DMSO}-d_6$  (A) and  $\text{D}_2\text{O}$  (B).

$^1\text{H}$  NMR in selective solvents allows us to evidence the core–shell structure of micelles prepared from amphiphilic block copolymers. Water is able to dissolve the hydrophilic block, that is, the shell block of micelles, but not the hydrophobic block. Thus, only the signals corresponding to HPMC are visible on the NMR spectrum in deuterated water. As shown in Figure 2B, signals belonging to PCL blocks are not observed due to their limited movement. This finding well corroborates with the micelle structure composed of a hydrophilic HPMC shell and a hydrophobic PCL core.

DOSY-NMR was also used to evidence the synthesis of HPMC–PCL block copolymers. The DOSY-NMR spectrum is a 2D diagram: one dimension shows the chemical shift, and the other dimension provides separation based on the self-diffusion coefficients of the dissolved species.<sup>40,41</sup> As shown in Figure 3, all the signals corresponding to PCL and HPMC are detected at the same diffusion coefficient. This finding suggests that the both blocks are combined in the same polymer chain, thus confirming the successful synthesis of HPMC–PCL block copolymers.

**Figure 3.** DOSY-NMR spectrum of HPMC7K-PCL<sub>30</sub> in  $\text{DMSO}-d_6$ .

FT-IR was also used to analyze the chemical structure of HPMC–PCL copolymers and precursors (Figure 4). Boc-OH

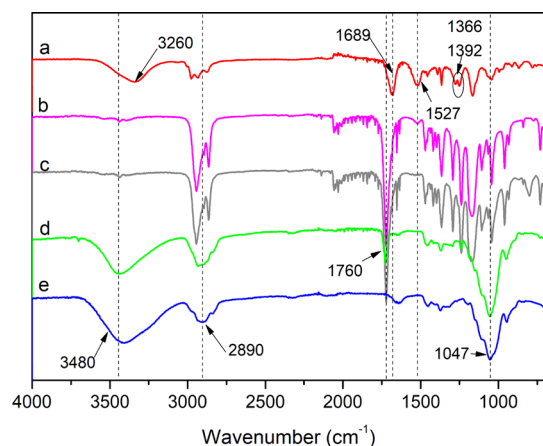


**Figure 4.** FT-IR spectra of Boc-OH (a), Boc-NH-PCL<sub>30</sub> (b), NH<sub>2</sub>-PCL<sub>30</sub> (c), HPMC7K-PCL<sub>30</sub> (d), and HPMC7K (e).

presents characteristic absorption bands at 3260, 1689, 1527, 1392, and 1366 cm<sup>-1</sup> which belong to O–H, C=O, CO–NH, and C–H (methyl) groups, respectively. These bands become less intense on the spectrum of Boc-NH-PCL and invisible on the spectrum of NH<sub>2</sub>-PCL because of the deprotection. The carbonyl band of PCL is detected at 1760 cm<sup>-1</sup>. On the spectrum of HPMC, absorption bands of O–H, C–H, and C–O bonds are detected at 3480, 2890, and 1047 cm<sup>-1</sup>, respectively. Signals corresponding to both HPMC and PCL are observed on the spectrum of HPMC7K-PCL<sub>30</sub>, which corroborates with the presence of both blocks in the copolymer.

### 3.2. Self-Assembly of Amphiphilic Block Copolymers.

HPMC–PCL amphiphilic block copolymers are able to self-assemble into nanoscale micelles with the shell–core structure by direct dissolution in water. The self-assembly properties of copolymers were investigated by means of DLS, TEM, and fluorescence spectroscopy.

The CMC is a key parameter of self-assembled polymeric micelles. Fluorescence spectroscopy allowed determination of the CMC of copolymers, using pyrene as the fluorescent probe. Once hydrophobic association of copolymer chains occurs in the aqueous medium, pyrene molecules significantly migrate into hydrophobic regions, resulting in changes of its photo-physical properties.<sup>42</sup> As shown in Figure 5A, the red shift of

absorption indicates pyrene migration into the nonpolar core of micelles, in agreement with micelle formation. The CMC is derived from the two tangent lines of the intensity ratio of  $I_{336}/I_{334}$  versus polymer concentration plots (Figure 5B). As summarized in Table 1, the CMC decreases from 0.012 for HPMC7K-PCL<sub>10</sub> to 0.0009 g/L for HPMC7K-PCL<sub>30</sub> and from 0.009 for HPMC18K-PCL<sub>10</sub> to 0.003 g/L for HPMC18K-PCL<sub>30</sub>. Therefore, longer hydrophobic block or shorter hydrophilic block facilitates micelle formation, thus leading to lower CMC, as reported in literature.<sup>43–45</sup>

The micelle size, size distribution, and zeta potential of micelles are determined by DLS. The diameter of HPMC7K-PCL micelles is in the range of 179.0–195.9 nm with a narrow polydispersity index (PDI) from 0.12 to 0.17 (Table 1). The size of HPMC18K-PCL micelles ranges from 205.1 to 222.0 nm that is larger than that of HPMC7K-PCL ones, suggesting that longer hydrophilic blocks yield larger micelles. It is also noticed that the micelle size is only slightly affected by the hydrophobic PCL block length. The zeta potential of micelles is slightly negative because there are no charged groups at the surface of the HPMC shell (Table 1). The morphology of micelles was visualized by TEM, as shown in Figure 6B. Spherical micelles are observed in all cases. The diameter of micelles by TEM ranges from 50 to 100 nm that is smaller than that obtained by DLS. This difference could be attributed to dehydration of micelles during TEM observation.<sup>23</sup>

### 3.3. Drug Loading and In Vitro Drug Release.

Curcumin was selected as the lipophilic model drug to assess the drug loading and release behaviors of HPMC–PCL copolymer micelles. Curcumin is a wide spectrum chemotherapeutic drug with outstanding antiproliferative and proapoptotic activities. In addition, it has been demonstrated that curcumin is able to regulate the intracellular levels of ATP-binding cassette drug transporters, which helps to prevent multidrug resistance.

Curcumin-loaded micelles were prepared using a two-step procedure: direct dissolution of block copolymers in water to yield blank micelles, followed by introduction of a curcumin solution in ethanol into the micelle solution. As shown in Table 1, the DLC and DLE are higher for HPMC–PCL micelles with longer hydrophobic PCL blocks. In the case of the HPMC7K-PCL series, the DLC increases from 4.3% for HPMC7K-PCL<sub>10</sub> to 8.2% for HPMC7K-PCL<sub>30</sub>, whereas the DLE increases from 41.5% for HPMC7K-PCL<sub>10</sub> to 75.8% for HPMC7K-PCL<sub>30</sub>. Similar phenomena are observed for HPMC18K-PCL copolymer micelles. Nevertheless, HPMC7K-PCL presents higher DLC and DLE than

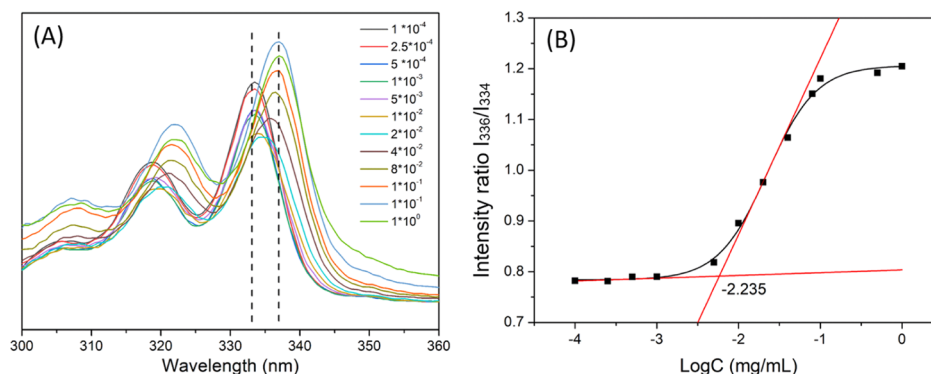


**Figure 5.** Fluorescence excitation spectra (A) and plot of intensity ratio  $I_{336}/I_{334}$  vs concentration (B) of HPMC7K-PCL<sub>20</sub> copolymer solutions.

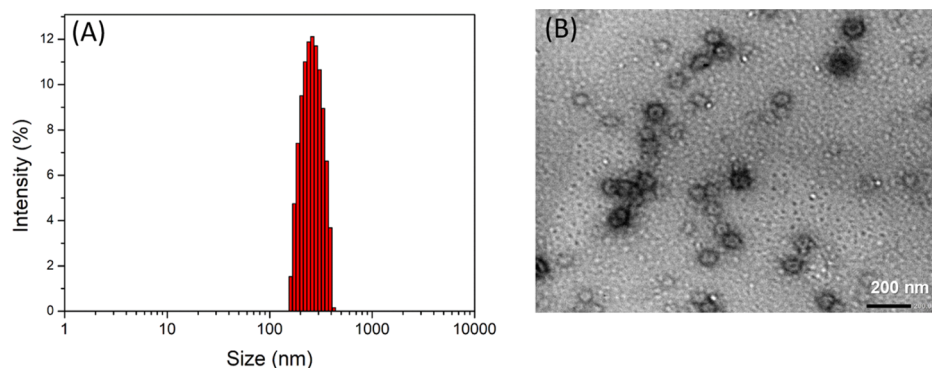


**Figure 6.** Size distribution by DLS (A) and TEM image (B) of HPMC7K-PCL<sub>20</sub> copolymer micelles.

HPMC18K-PCL with the same PCL block length. In other words, micelles with a higher hydrophobic/hydrophilic ratio present stronger encapsulation ability, as reported in literature. The DLC and DLE of curcumin encapsulated in PCL-PEG micelles increase from 15.9 to 20.6% and from 65.4 to 82.3%, respectively, with an increase of the PCL/PEG ratio from 2 to 5.<sup>46</sup> Nimodipine-loaded PCL-PEG-PCL micelles also present an enhanced DLC by increasing PCL/PEG ratio.<sup>44</sup> In the case of amiodarone-loaded PEG-PCL micelles, the DLC increases from 2.4 to 7.8% with increase of PCL molar mass from 5000 to 24,000.<sup>47</sup>

The increase of DLC and DLE with an increasing PCL block length can be attributed to the interaction between curcumin and the hydrophobic part of micelles. Gou *et al.* prepared curcumin-loaded nanoparticles derived from natural silk fibroin. Circular dichroism spectra showed that blank nanoparticles had much more  $\beta$ -structures than curcumin-loaded ones, which was assigned to interactions of curcumin with the hydrophobic domains of nanoparticles, hindering the formation of  $\beta$ -sheet structures.<sup>48</sup> In curcumin-loaded PCL-PEG micelles, the interface area between PCL and curcumin was estimated by simulation ten times larger than that between PEG and curcumin, suggesting that the main interaction occurs between hydrophobic PCL of the copolymer and hydrophobic curcumin.<sup>16</sup>

*In vitro* drug release was realized by using the dialysis method in pH 7.4 PBS at 37 °C. As shown in Figure 7, a biphasic release profile is observed for all curcumin-loaded micelles, including a rapid initial release within the first 6 h and

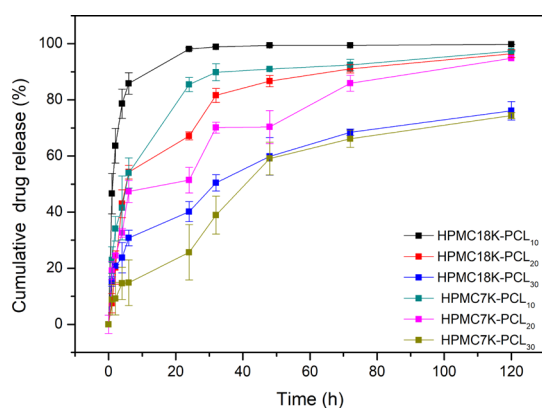


**Figure 7.** Cumulative release of curcumin from HPMC-PCL copolymer micelles. Data points represent mean  $\pm$  SD from triplicate samples, and error bars represent the standard deviation ( $n = 3$ ).

a slower release in the remaining period up to 120 h. The initial burst release could be attributed to the fact that a part of drug is located at the interface of the core-shell structure.<sup>49</sup> HPMC18K-PCL<sub>10</sub> presents the largest burst release of over 80% in the first 6 h, whereas HPMC7K-PCL<sub>30</sub> presents a burst of 15% only. The total release at 120 h is 99.8, 97.4, 94.9, and 96.5% for HPMC18K-PCL<sub>10</sub>, HPMC18K-PCL<sub>20</sub>, HPMC7K-PCL<sub>10</sub>, and HPMC7K-PCL<sub>20</sub>, respectively. In contrast, the total release at 120 h is 74.4% for HPMC7K-PCL<sub>30</sub> and 76.1% for HPMC18K-PCL<sub>30</sub>, which is much lower than those of copolymers with a shorter PCL block length. Therefore, the release rate and release percentage from HPMC-PCL copolymer micelles is dependent on the hydrophobic block length and the hydrophobic/hydrophilic ratio. The longer hydrophobic block, the larger the hydrophobic/hydrophilic ratio, the lower the release rate. It should also be noted that micelles with longer hydrophobic block have higher drug load. Hu *et al.* reported that curcumin-loaded P(NIPAAm-co-DMAAm)-*b*-PLLA copolymer micelles with a higher drug load present a slower release rate compared to those with a lower drug load.<sup>50</sup> Therefore, the release rate is also dependent on the DLC because drug solubility in the medium could be a limiting factor which significantly affects drug release. Sink conditions are often used to minimize the effect of drug solubility. Nimodipine-loaded PCL-PEG-PCL micelles also present a decrease of the drug release rate with the increase of the PCL block length.<sup>44</sup> Similarly, Danafar *et al.* reported that curcumin release from PCL-PEG micelles in 120 h decreases from 80.2 to 57.1% with the CL/EG ratio increase from 2 to 5.<sup>46</sup>

**3.4. Biocompatibility of Micelles.** The MTT test was applied to assess the cytocompatibility of HPMC-PCL micelles on L929 cells. MTT can react with succinate mitochondrial dehydrogenases which are present in living cells to yield formazan, a purple dye. The latter is insoluble in water but soluble in DMSO. Thus, the absorbance of formazan in DMSO solution is measured to assess the number of living cells.

L-929 cells are a commonly used murine fibroblast cell line for cytocompatibility evaluation. Figure 8 shows the relative activity of L929 cells after culture with HPMC7K-PCL<sub>10</sub> and HPMC7K-PCL<sub>20</sub> micelle solutions at various concentrations. The viability of cells is well above 80% in the whole concentration range. After 72 h incubation, the cell viability is around 90% in all cases. These results indicate that HPMC-PCL copolymer micelles are well compatible with L-929 cells.

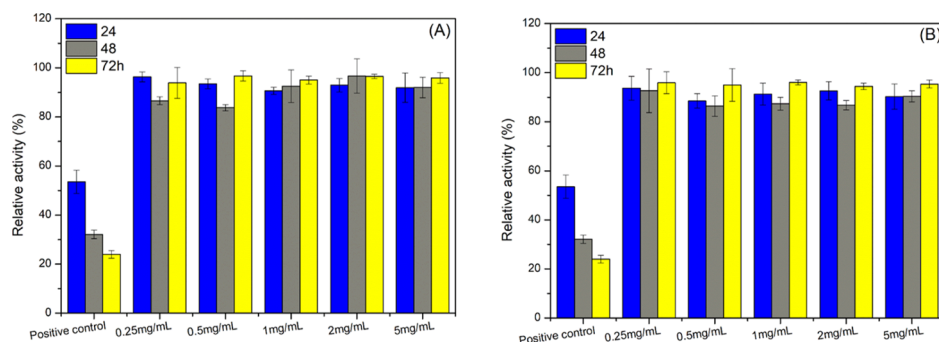


**Figure 8.** Relative activity of L-929 cells after 24, 48, and 72 h culture with HPMC7K-PCL<sub>10</sub> (A) and HPMC7K-PCL<sub>20</sub> (B) micelle solutions at different concentrations in comparison with the positive control. Data are presented as the mean  $\pm$  sd ( $n = 3$ ).

#### 4. CONCLUSIONS

In this work, a series of biobased amphiphilic HPMC-PCL block copolymers were synthesized by reductive amination between the hemiacetal reducing endgroup of HPMC and end functionalized PCL. The copolymers and precursors were characterized by NMR, DOSY-NMR, FT-IR, GPC, and the Kaiser test. The self-assembly of copolymers was evidenced by fluorescence spectroscopy, DLS, and TEM measurements. All the copolymers are able to self-assemble in water into spherical nanoscale micelles with narrow distribution. The longer hydrophilic HPMC block leads to a larger micelle size. The CMC of copolymers decreases with an increasing hydrophobic PCL block length. Curcumin was successfully encapsulated in the micelle core as a lipophilic anticancer drug. Higher drug loading was obtained for copolymers with a longer PCL block length. The drug release rate is dependent on the PCL block length and drug load. The larger PCL block length or a higher drug load leads to slower drug release. The MTT test shows that HPMC-PCL micelles present outstanding cytocompatibility. In conclusion, biocompatible and biodegradable HPMC-PCL block copolymers could present great potential as nanocarriers of lipophilic drugs.

#### ■ ASSOCIATED CONTENT

Characterization of Boc-NH-PCL polymers by NMR and GPC, GPC curves of Boc-NH-PCL<sub>30</sub> and NH<sub>2</sub>-PCL<sub>30</sub> in THF, and the Kaiser test of Boc-NH-PCL<sub>30</sub>, NH<sub>2</sub>-PCL<sub>30</sub>, and HPMC7K-PCL<sub>30</sub> ([PDF](#))

#### ■ AUTHOR INFORMATION

##### Corresponding Author

**Suming Li** – Institut Européen des Membranes, IEM UMR 5635, Univ Montpellier, CNRS, ENSCM, Montpellier 34095, France; [orcid.org/0000-0002-3345-1479](https://orcid.org/0000-0002-3345-1479); Email: [suming.li@umontpellier.fr](mailto:suming.li@umontpellier.fr)

##### Authors

**Aijing Lu** – Institut Européen des Membranes, IEM UMR 5635, Univ Montpellier, CNRS, ENSCM, Montpellier 34095, France  
**Eddy Petit** – Institut Européen des Membranes, IEM UMR 5635, Univ Montpellier, CNRS, ENSCM, Montpellier 34095, France

**Yuandou Wang** – Institute of High Performance Polymers, Qingdao University of Science and Technology, Qingdao 266042, China

**Feng Su** – Institute of High Performance Polymers, Qingdao University of Science and Technology, Qingdao 266042, China

#### ■ ACKNOWLEDGMENTS

This work is supported in part by the scholarship from the China Scholarship Council (grant CSC no. 201606240124) and the European Institute of Membranes (Exploratory project “Bisostent–Health” of the Internal Call 2017).

#### ■ REFERENCES

- (1) Cabral, H.; Miyata, K.; Osada, K.; Kataoka, K. Block Copolymer Micelles in Nanomedicine Applications. *Chem. Rev.* **2018**, *118*, 6844–6892.
- (2) Dash, T. K.; Konkimalla, V. B. Poly-small je, Ukrainian-caprolactone based formulations for drug delivery and tissue engineering: A review. *J. Controlled Release* **2012**, *158*, 15–33.
- (3) Grossen, P.; Witzigmann, D.; Sieber, S.; Huwyler, J. PEG-PCL-based nanomedicines: A biodegradable drug delivery system and its application. *J. Controlled Release* **2017**, *260*, 46–60.
- (4) Karami Ghaleseidi, Z.; Dadkhah Tehrani, A.; Parsamanesh, M. Starch-based dual amphiphilic graft copolymer as a new pH-sensitive multidrug co-delivery system. *Int. J. Biol. Macromol.* **2018**, *118*, 913–920.
- (5) Liu, L.; Wang, Y.; Shen, X.; Fang, Y. e. Preparation of chitosan-g-polycaprolactone copolymers through ring-opening polymerization of epsilon-caprolactone onto phthaloyl-protected chitosan. *Biopolymers* **2005**, *78*, 163–170.
- (6) Youssouf, L.; Bhaw-Luximon, A.; Diotel, N.; Catan, A.; Giraud, P.; Gimié, F.; Koshel, D.; Casale, S.; Bénard, S.; Meneyrol, V.; Lallemand, L.; Meilhac, O.; Lefebvre D’Hellencourt, C.; Jhurry, D.; Couprie, J. Enhanced effects of curcumin encapsulated in poly-caprolactone-grafted oligocarrageenan nanomicelles, a novel nanoparticle drug delivery system. *Carbohydr. Polym.* **2019**, *217*, 35–45.
- (7) Irani, M.; Mir Mohamad Sadeghi, G.; Haririan, I. Gold coated poly (epsilon-caprolactonediol) based polyurethane nanofibers for controlled release of temozolomide. *Biomed. Pharmacother.* **2017**, *88*, 667–676.
- (8) Sinha, V. R.; Bansal, K.; Kaushik, R.; Kumria, R.; Trehan, A. Poly-epsilon-caprolactone microspheres and nanospheres: an overview. *Int. J. Pharm.* **2004**, *278*, 1–23.

- (9) Hakkarainen, M.; Albertsson, A.-C. Heterogeneous biodegradation of polycaprolactone - low molecular weight products and surface changes. *Macromol. Chem. Phys.* **2002**, *203*, 1357–1363.
- (10) Qiu, L. Y.; Bae, Y. H. Self-assembled polyethylenimine-graft-poly(epsilon-caprolactone) micelles as potential dual carriers of genes and anticancer drugs. *Biomaterials* **2007**, *28*, 4132–4142.
- (11) Ahmed, F.; Discher, D. E. Self-porating polymersomes of PEG-PLA and PEG-PCL: hydrolysis-triggered controlled release vesicles. *J. Controlled Release* **2004**, *96*, 37–53.
- (12) Gu, C.; Le, V.; Lang, M.; Liu, J. Preparation of polysaccharide derivatives chitosan-graft-poly(varepsilon-caprolactone) amphiphilic copolymer micelles for 5-fluorouracil drug delivery. *Colloids Surf., B* **2014**, *116*, 745–750.
- (13) Shuai, X.; Merdan, T.; Schaper, A. K.; Xi, F.; Kissel, T. Core-cross-linked polymeric micelles as paclitaxel carriers. *Bioconjugate Chem.* **2004**, *15*, 441–448.
- (14) Ge, H.; Hu, Y.; Jiang, X.; Cheng, D.; Yuan, Y.; Bi, H.; Yang, C. Preparation, characterization, and drug release behaviors of drug nimodipine-loaded poly( $\epsilon$ -caprolactone)-poly(ethylene oxide)-poly( $\epsilon$ -caprolactone) amphiphilic triblock copolymer micelles. *J. Pharm. Sci.* **2002**, *91*, 1463–1473.
- (15) Tang, X.; Lyu, Y.; Xie, D.; Li, A.; Liang, Y.; Zheng, D. Therapeutic Effect of Sorafenib-Loaded TPGS-b-PCL Nanoparticles on Liver Cancer. *J. Biomed. Nanotechnol.* **2018**, *14*, 396–403.
- (16) Peng, J.-R.; Qian, Z.-Y. Drug delivery systems for overcoming the bioavailability of curcumin: not only the nanoparticle matters. *Nanomedicine* **2014**, *9*, 747–750.
- (17) Qi, M.; Zou, S.; Guo, C.; Wang, K.; Yu, Y.; Zhao, F.; Fan, H.; Wu, Z.; Liu, W.; Chen, D. Enhanced In Vitro and In Vivo Anticancer Properties by Using a Nanocarrier for Co-Delivery of Antitumor Polypeptide and Curcumin. *J. Biomed. Nanotechnol.* **2018**, *14*, 139–149.
- (18) Liu, Z.; Jiao, Y.; Wang, Y.; Zhou, C.; Zhang, Z. Polysaccharides-based nanoparticles as drug delivery systems. *Adv. Drug Delivery Rev.* **2008**, *60*, 1650–1662.
- (19) Klemm, D.; Heublein, B.; Fink, H.-P.; Bohn, A. Cellulose: fascinating biopolymer and sustainable raw material. *Angew. Chem., Int. Ed. Engl.* **2005**, *44*, 3358–3393.
- (20) Moon, R. J.; Martini, A.; Nairn, J.; Simonsen, J.; Youngblood, J. Cellulose nanomaterials review: structure, properties and nanocomposites. *Chem. Soc. Rev.* **2011**, *40*, 3941–3994.
- (21) Yang, J.; Li, J. Self-assembled cellulose materials for biomedicine: A review. *Carbohydr. Polym.* **2018**, *181*, 264–274.
- (22) Al-Tabakha, M. M. HPMC capsules: current status and future prospects. *J. Pharm. Pharm. Sci.* **2010**, *13*, 428–442.
- (23) Bordallo, E.; Rieumont, J.; Tiera, M. J.; Gómez, M.; Lazzari, M. Self-assembly in aqueous solution of amphiphilic graft copolymers from oxidized carboxymethylcellulose. *Carbohydr. Polym.* **2015**, *124*, 43–49.
- (24) Wang, D.; Tan, J.; Kang, H.; Ma, L.; Jin, X.; Liu, R.; Huang, Y. Synthesis, self-assembly and drug release behaviors of pH-responsive copolymers ethyl cellulose-graft-PDEAEMA through ATRP. *Carbohydr. Polym.* **2011**, *84*, 195–202.
- (25) Das, R.; Pal, S. Hydroxypropyl methyl cellulose grafted with polyacrylamide: application in controlled release of 5-amino salicylic acid. *Colloids Surf., B* **2013**, *110*, 236–241.
- (26) Lu, A.; Wang, J.; Najarro, M. C.; Li, S.; Deratani, A. Synthesis and self-assembly of AB<sub>2</sub>-type amphiphilic copolymers from biobased hydroxypropyl methyl cellulose and poly(L-lactide). *Carbohydr. Polym.* **2019**, *211*, 133–140.
- (27) Wang, J.; Caceres, M.; Li, S.; Deratani, A. Synthesis and Self-Assembly of Amphiphilic Block Copolymers from Biobased Hydroxypropyl Methyl Cellulose and Poly(L-lactide). *Macromol. Chem. Phys.* **2017**, *218*, 1600558.
- (28) Lu, A.; Petit, E.; Li, S.; Wang, Y.; Su, F.; Monge, S. Novel thermo-responsive micelles prepared from amphiphilic hydroxypropyl methyl cellulose-block-JEFFAMINE copolymers. *Int. J. Biol. Macromol.* **2019**, *135*, 38–45.
- (29) Lu, A.; Petit, E.; Jelonek, K.; Orchel, A.; Kasperczyk, J.; Wang, Y.; Su, F.; Li, S. Self-assembled micelles prepared from bio-based hydroxypropyl methyl cellulose and polylactide amphiphilic block copolymers for anti-tumor drug release. *Int. J. Biol. Macromol.* **2020**, *154*, 39–47.
- (30) ten Breteler, M. R.; Feijen, J.; Dijkstra, P. J.; Signori, F. Synthesis and thermal properties of hetero-bifunctional PLA oligomers and their stereocomplexes. *React. Funct. Polym.* **2013**, *73*, 30–38.
- (31) Le Hellaye, M.; Fortin, N.; Guilloteau, J.; Soum, A.; Lecommandoux, S.; Guillaume, S. M. Biodegradable polycarbonate-b-polypeptide and polyester-b-polypeptide block copolymers: synthesis and nanoparticle formation towards biomaterials. *Biomacromolecules* **2008**, *9*, 1924–1933.
- (32) Moussa, A.; Crépet, A.; Ladavière, C.; Trombotto, S. Reducing-end “clickable” functionalizations of chitosan oligomers for the synthesis of chitosan-based diblock copolymers. *Carbohydr. Polym.* **2019**, *219*, 387–394.
- (33) Abdel-Magid, A. F.; Mehrman, S. J. A review on the use of sodium triacetoxymethylborohydride in the reductive amination of ketones and aldehydes. *Org. Process Res. Dev.* **2006**, *10*, 971–1031.
- (34) Trent, J. S. Ruthenium Tetraoxide Staining of Polymers - New Preparative Methods for Electron-Microscopy. *Macromolecules* **1984**, *17*, 2930–2931.
- (35) Fielding, L. A.; Derry, M. J.; Ladmiraal, V.; Rosselgong, J.; Rodrigues, A. M.; Ratcliffe, L. P. D.; Sugihara, S.; Armes, S. P. RAFT dispersion polymerization in non-polar solvents: facile production of block copolymer spheres, worms and vesicles in n-alkanes. *Chem. Sci.* **2013**, *4*, 2081.
- (36) Hu, Y.; Darcos, V.; Monge, S.; Li, S. Thermo-responsive drug release from self-assembled micelles of brush-like PLA/PEG analogues block copolymers. *Int. J. Pharm.* **2015**, *491*, 152–161.
- (37) Trache, D.; Hussin, M. H.; Hui Chuin, C. T.; Sabar, S.; Fazita, M. R. N.; Taiwo, O. F. A.; Hassan, T. M.; Haafiz, M. K. M. Microcrystalline cellulose: Isolation, characterization and biocomposites application-A review. *Int. J. Biol. Macromol.* **2016**, *93*, 789–804.
- (38) Ju, M.; Gong, F.; Cheng, S.; Gao, Y. Fast and Convenient Synthesis of Amine-Terminated Polylactide as a Macroinitiator for  $\omega$ -Benzoyloxycarbonyl-L-Lysine-N-Carboxyanhydrides. *Int. J. Polym. Sci.* **2011**, *2011*, 1–7.
- (39) Gotsche, M.; Keul, H.; Höcker, H. Amino-terminated poly(L-lactide)s as initiators for the polymerization of N-carboxyanhydrides: synthesis of poly(L-lactide)-block-poly( $\alpha$ -amino acid)s. *Macromol. Chem. Phys.* **1995**, *196*, 3891–3903.
- (40) Pagès, G.; Gilard, V.; Martino, R.; Malet-Martino, M. Pulsed-field gradient nuclear magnetic resonance measurements (PFG NMR) for diffusion ordered spectroscopy (DOSY) mapping. *Analyst* **2017**, *142*, 3771–3796.
- (41) Jiang, Z.; Blakey, I.; Whittaker, A. K. Aqueous solution behaviour of novel water-soluble amphiphilic copolymers with elevated hydrophobic unit content. *Polym. Chem.* **2017**, *8*, 4114–4123.
- (42) Li, J.; Yang, J. Synthesis of folate mediated carboxymethyl cellulose fatty acid ester and application in drug controlled release. *Carbohydr. Polym.* **2019**, *220*, 126–131.
- (43) Hu, Y.; Jiang, X.; Ding, Y.; Zhang, L.; Yang, C.; Zhang, J.; Chen, J.; Yang, Y. Preparation and drug release behaviors of nimodipine-loaded poly( $\epsilon$ -caprolactone)-poly(ethylene oxide)-polylactide amphiphilic copolymer nanoparticles. *Biomaterials* **2003**, *24*, 2395–2404.
- (44) Ge, H.; Hu, Y.; Jiang, X.; Cheng, D.; Yuan, Y.; Bi, H.; Yang, C. Preparation, characterization, and drug release behaviors of drug nimodipine-loaded poly( $\epsilon$ -caprolactone)-poly(ethylene oxide)-poly( $\epsilon$ -caprolactone) amphiphilic triblock copolymer micelles. *J. Pharm. Sci.* **2002**, *91*, 1463–1473.
- (45) Yang, H.; Wang, N.; Mo, L.; Wu, M.; Yang, R.; Xu, X.; Huang, Y.; Lin, J.; Zhang, L.-M.; Jiang, X. Reduction sensitive hyaluronan-SS-poly(epsilon-caprolactone) block copolymers as theranostic nano-

carriers for tumor diagnosis and treatment. *Mater. Sci. Eng., C* **2019**, *98*, 9–18.

(46) Kheiri Manjili, H.; Ghasemi, P.; Malvandi, H.; Mousavi, M. S.; Attari, E.; Danafar, H. Pharmacokinetics and in vivo delivery of curcumin by copolymeric mPEG-PCL micelles. *Eur. J. Pharm. Biopharm.* **2017**, *116*, 17–30.

(47) Elhasi, S.; Astaneh, R.; Lavasanifar, A. Solubilization of an amphiphilic drug by poly(ethylene oxide)-block-poly(ester) micelles. *Eur. J. Pharm. Biopharm.* **2007**, *65*, 406–413.

(48) Gou, S.; Huang, Y.; Wan, Y.; Ma, Y.; Zhou, X.; Tong, X.; Huang, J.; Kang, Y.; Pan, G.; Dai, F.; Xiao, B. Multi-bioresponsive silk fibroin-based nanoparticles with on-demand cytoplasmic drug release capacity for CD44-targeted alleviation of ulcerative colitis. *Biomaterials* **2019**, *212*, 39–54.

(49) Tyrrell, Z. L.; Shen, Y.; Radosz, M. Fabrication of micellar nanoparticles for drug delivery through the self-assembly of block copolymers. *Prog. Polym. Sci.* **2010**, *35*, 1128–1143.

(50) Hu, Y.; Darcos, V.; Monge, S.; Li, S.; Zhou, Y.; Su, F. Thermo-responsive release of curcumin from micelles prepared by self-assembly of amphiphilic P(NIPAAm-co-DMAAm)-b-PLLA-b-P-(NIPAAm-co-DMAAm) triblock copolymers. *Int. J. Pharm.* **2014**, *476*, 31–40.